

Coherence Length of Excitons in a Semiconductor Quantum Well

Hui Zhao, Sebastian Moehl, and Heinz Kalt

Institut für Angewandte Physik, Universität Karlsruhe, D-76128 Karlsruhe, Germany

We report on the first experimental determination of the coherence length of excitons in semiconductors using the combination of spatially resolved photoluminescence with phonon sideband spectroscopy. The coherence length of excitons in ZnSe quantum wells is determined to be $300 \sim 400$ nm, about $25 \sim 30$ times the exciton de Broglie wavelength. With increasing exciton kinetic energy, the coherence length decreases slowly. The discrepancy between the coherence lengths measured and calculated by only considering the acoustic phonon scattering suggests an important influence of static disorder.

Coherence is an essential intrinsic property of quantum-mechanical particles. A particle is called coherent if it propagates like a wave packet with well defined phases for its spectral components. Such particles have properties quite different from classical particles like the ability to show interference. Constructive interference leads to a macroscopic coherence of an ensemble of particles. This has profound consequences as is illustrated by the properties of laser radiation (coherent ensemble of photons) or by the formation of a new state of matter in a Bose-Einstein condensate (coherent ensemble of atoms). The coherence of such an ensemble is destroyed by phase relaxing processes of individual ensemble members. The temporal and spatial scales of phase-destroying processes are given by the particle coherence time and length, respectively.

The above arguments also hold for excitons, which are the fundamental quasi-particles of optical excitation in semiconductors. Recently, coherent control of both ensemble excitons[1] and individual excitons[2] has been demonstrated, making excitons possible candidates for quantum-information processing.[3] So it is important to study the coherence time and length of excitons, which define an upper temporal and spatial limit for coherent manipulations. Even for spin manipulations, the temporal or spatial de-coherence can influence spin coherence whenever spin-orbit coupling is present.[4] In this letter we present the first experimental determination of the coherence length of excitons in semiconductors.

Excitonic coherence is temporally and spatially limited due to interactions within the exciton ensemble and its coupling to its environment. We can divide these interactions into two classes: elastic and inelastic scattering. They have essentially different influences on the excitonic coherence.[5] For elastic scattering, the direction of the wave vector changes, but the energy of the exciton keeps constant. Consequently, the elastic scattering does not destroy the phase of the exciton. The spatial distribution of the wavefunction remains independent of time even after several elastic scattering events. Thus, the exciton wavefunction remains coherent.[5] One can find an analogue of this coherent propagation in the presence of elastic scattering in Anderson localization of electrons in

metals.[6] On the contrary, an inelastic scattering event changes the exciton energy and phase and thus destroys the coherence.

It is nowadays well established to measure the excitonic coherence time e.g. from the decay of the macroscopic optical polarization using ultrafast spectroscopy[7] or from the homogeneous linewidth of exciton luminescence[8]. Methods to investigate spatially coherent phenomena are much less developed. They require not only a spatial resolution on the order of the light wavelength[9, 10] but also a means to simultaneously test the coherence of the excitons. First attempts towards this goal were based on time- and space-resolved pump-probe experiments.[11, 12] But since the nonlinear response of the semiconductor was tested, only high-density regimes beyond the excitonic phase were accessible. We will show in this letter, that we are able to investigate the spatial coherence and measure the coherence length of excitons using spatially resolved phonon sideband spectroscopy in quantum-wells based on the polar semiconductor ZnSe.

The investigations require both specific material properties and a novel experimental design. The material of choice is a ZnSe/ZnSSe multiple quantum well for two reasons. Firstly, due to the strong Fröhlich coupling in polar II-VI quantum structures, one can optically generate well defined hot excitons assisted by the emission of longitudinal optical (LO)-phonons within some 100 fs,[13] as shown in Fig. 1. The initial kinetic energy of the exciton can be well controlled over a range of 30 meV simply by choosing the laser excitation energy, E_{exc} . This exciton formation mechanism is drastically different from that of III-V structures[14], in which most of the optically generated electrons and holes relax individually toward their respective band extrema, and bind to excitons on a time scale of 10 ps.[15] Secondly, the strong Fröhlich coupling induces a pronounced LO-phonon sideband (PSB) beside the zero-phonon-line (ZPL) in the photoluminescence (PL) spectrum. After their formation, the hot excitons relax to the band minimum by phonon emission. After relaxation, the cold excitons with nearly zero kinetic energy can radiatively recombine, resulting in the ZPL. Since the photon momentum is very small, this direct coupling to photons is

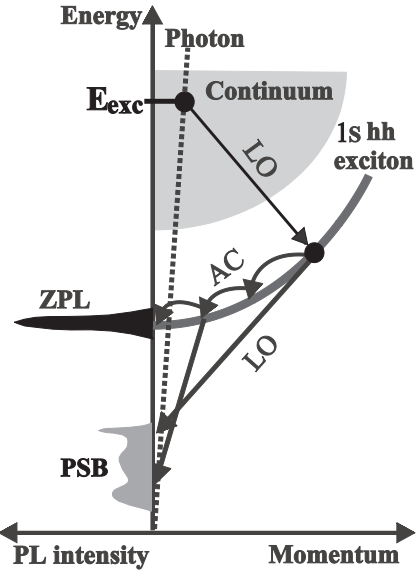


FIG. 1: Schematic drawing of the exciton formation assisted by LO-phonon emission, the subsequent relaxation by acoustic phonon (AC) emission and the resulting zero-phonon-line (ZPL) and phonon sideband (PSB).

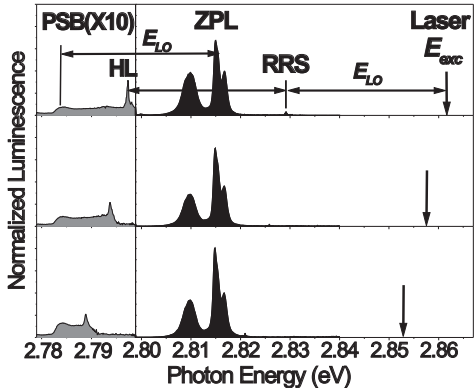


FIG. 2: Photoluminescence spectra measured at 7 K. The excitation intensity is $1 \text{ kW}/\text{cm}^2$.

forbidden for hot excitons due to momentum conservation. This is the main obstacle of hot exciton studies in conventional PL spectroscopy, which exploits the ZPL. For the same reason, the hot excitons are not observable in pump-probe experiments. However, the LO-phonon can assist the hot exciton in coupling with a photon by taking away its momentum (see Fig. 1). The simultaneous well-defined energy loss to the LO-phonon leads to the appearance of the PSB. This process is an ideal tool for the *direct* investigation of hot excitons.[13, 16]

Figure 2 shows three spectra excited by a continuous-wave laser at various photon energies E_{exc} . The PSB is found in the photon-energy range between one LO-phonon energy ($E_{LO}=31.8 \text{ meV}$) below the ZPL and

$2E_{LO}$ below the E_{exc} (see Fig. 2). The latter energy defines the upper limit of the PSB, which stays a strict limit when E_{exc} is varied. This fact confirms that the PSB really reflects the hot exciton distribution and that no additional luminescence, e.g., related to defects, occurs in this spectral range. In Fig. 2, a sharp peak (HL) is observed at $2E_{LO}$ below E_{exc} . This peak is the main subject of the present investigation. In the following we will identify its origin and discuss what we can learn from this peak.

Generally, the peak observed at $E_{exc} - nE_{LO}$ can be induced by hot exciton luminescence (HL) and/or resonant Raman scattering (RRS).[17] There has been a debate in the 1970's how to distinguish these two processes.[18, 19, 20, 21] The actual difference between them is whether a real excitonic population is involved or not.[18] HL is composed of two distinct one-photon processes, i.e., absorption followed by emission, while RRS is a single two-photon process.[22] In the case of $n = 1$, HL is not possible,[17] thus the peak can be easily identified as a first order RRS. Indeed, this peak is observed in Fig. 2 on the high energy side of the ZPL. In the cases of $n \geq 2$, both HL and RRS are possible. In experiments, one can distinguish them according to their different features.[17]. Recently, it has been proven that HL can be the dominant process at low temperature in several systems, e.g., II-VI[22, 23, 24, 25], III-V[26] and IV-IV[27] semiconductors. In our experiments, we prove that the sharp peak observed at the upper limit of PSB is dominated by HL by the following experimental facts. At first, raising the temperature we observe a pronounced thermal quenching of this peak (from 800 counts at 10 K to less than 100 counts at 70 K), while the RRS peak keeps unchanged in this temperature range (about 160 counts). Such different temperature behaviors clearly distinguish HL and RRS. [17, 27] Secondly, increasing the photon energy of excitation by one LO-phonon energy, i.e., moving the E_{exc} from the range ($E_{ZPL} + E_{LO}$, $E_{ZPL} + 2E_{LO}$) to ($E_{ZPL} + 2E_{LO}$, $E_{ZPL} + 3E_{LO}$), the spectral linewidth of the HL peak becomes $2 \sim 3$ times wider. If the peak were dominated by RRS process, such an increase of the E_{exc} corresponds to a change from second order RRS to third order RRS. In this case the linewidth should be constant.[23] On the other hand, if the peak was induced by HL process, the above tuning of the E_{exc} introduces an additional relaxation step by LO-phonon emission before the LO-phonon assisted recombination, thus broaden the linewidth, as has been observed in ZnTe quantum wells.[23] Beside these facts, the different spatial profiles of the HL and RRS peaks (see below) also provides evidence of their origins.

Having excluded a significant Raman contribution to the HL peak, we will see that the peak can be exploited to study the individual coherence of excitons. The peak is spectrally located at $2E_{LO}$ below E_{exc} thus $1E_{LO}$ below the exciton initial kinetic energy. So it actually monitors

the population of excitons right after their LO–phonon assisted formation and before their first inelastic scattering event. An exciton that has undergone the first inelastic scattering event, thus has a different energy, cannot contribute to the peak. Since an exciton remains coherent between two inelastic scattering events, *the HL peak at $2E_{LO}$ below E_{exc} monitors the presence of individual coherent excitons* with a well defined kinetic energy $E_{exc} - E_{LO}$.

The experimental setup has to incorporate spatially narrow excitation and detection areas, with the latter being shiftable with respect to the former in a well defined way. These requirements are fulfilled by a solid immersion lens (SIL)-enhanced confocal micro-photoluminescence (μ -PL) system[28]. The system consists of a microscope objective ($20\times$, numerical aperture $NA = 0.4$) and a hemisphere SIL[29] of refractive index $n_r = 2.2$. The excitation source is a tunable continuous-wave Ti:sapphire laser pumped by an Ar–ion laser and frequency doubled using a BBO crystal. The laser beam is focused to a spot size of 400 nm (FWHM) on the sample by the objective. The luminescence at a lattice temperature of 7 K is collected by the same objective, and recorded by a cooled CCD camera attached to a high-resolution spectrometer. A 20 μ m pinhole in the image plane of the microscope selects the detection area. The SIL is adhesively fixed to the sample surface, improving the spatial resolution by a factor of n_r . We confirm the overall resolution of the whole system including pinhole to be about 450 nm (FWHM). Furthermore, the introduction of the SIL leads to an enhancement of the PL collection efficiency by more than four times, close to the theoretical limit (5.6 times) in our setup.

Although the spatial resolution of this system is lower than that of a scanning near field optical microscope (SNOM) using coated fiber tips, the collection efficiency is much higher than for the latter. Since the PSB is much weaker than the ZPL (see Fig. 2), a high collection efficiency is paramount for the investigation of the coherent exciton behavior using the PSB. Similar collection efficiencies are achieved when the SNOM includes an uncoated fiber tip.[30] But a SNOM experiment has a second disadvantage: one cannot detect spatially resolved spectra from positions outside the excitation spot. In contrast, moving the pinhole in the image plane of the SIL-enhanced μ -PL enables us to investigate the spatial coherence of excitons in a rather direct way. Further, using a PL setup, we have access to the low-density regime where exciton–exciton interactions are negligible. This is not the case for pump–probe type experiments using SIL or nano-apertures [11, 12].

By scanning the pinhole, we measure the spectra of the PSB at different detection positions with respect to the excitation spot, as shown in Fig. 3(a). We find the HL peak drops with increasing the excitation–detection distance, but is still visible at a distance as large as

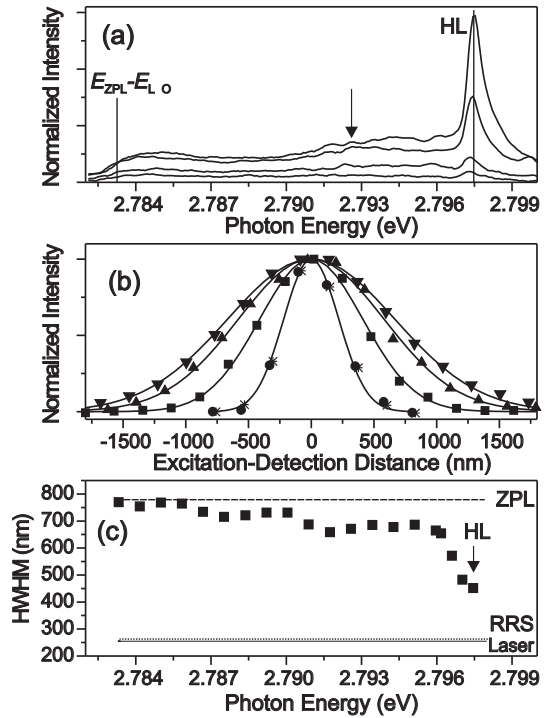


FIG. 3: (a) Spectra of PSB measured at different positions with respect to the excitation–laser spot. The distances from the excitation spot to the detection spot are (from top to bottom) 0, 460, 920 and 1380 nm, respectively. The excitation laser energy is 2.8611 eV, with intensity of 1 kW/cm². (b) Spatial profiles of the excitation–laser spot (circles), RRS (stars), HL (squares) and ZPL (down–triangles). The spatial profile of one spectral component in the PSB, indicated as the arrow in (a), is also shown as the up–triangles. The solid lines represent the corresponding Gaussian fits to the data. (c) HWHM of the spectral components in the PSB as function of the photon energy. The HWHMs are obtained by Gaussian fits of the spatial profiles of the selected components. The HWHMs of the ZPL (dashed), RRS (dots) and laser (solid) are also shown for comparison.

1380 nm. We also find a systematic change of the PSB spectral shape, which reflects the relaxation of the hot excitons during transport. These spectra allow us to obtain the spatial profile of the HL peak, as shown by the squares in Fig. 3(b). We also plot in the same figure the spatial profiles of the laser spot (circles), the RRS peak (stars) and the ZPL (down–triangles) measured in the same pinhole–scanning. The profile of RRS peak is similar to that of the laser spot, while the HL peak distribution is significantly wider. We note that the difference in spatial extension can also be used as a method to distinguish the HL and RRS processes. We also check the spatial profile of a spectral component in the middle part of the PSB, as indicated by the arrow in Fig. 3(a). The profile (up–triangles) locates between the HL and ZPL profiles, showing the undergoing relaxation. Such a feature is shown quantitatively in Fig. 3(c). Decreasing the

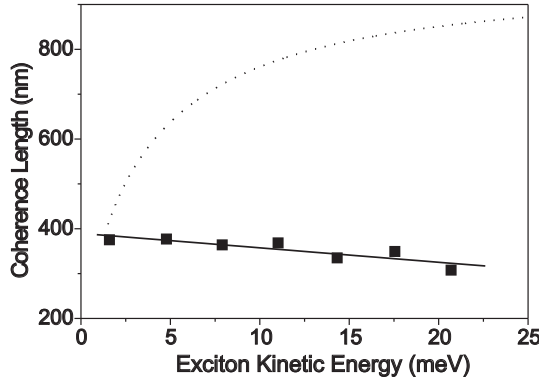


FIG. 4: Exciton coherence lengths (squares) deduced from the spatial profiles of the HL peaks for several exciton kinetic energies. The solid line is a guide for the eyes. Also shown is the calculated coherence length (dots) limited by acoustic phonon scattering without considering the influence of disorder.

detection energy from HL peak to $E_{ZPL} - E_{LO}$, i.e., scanning the arrow in Fig. 3(a) from right to left within the PSB, we find an increase of the HWHM (half-width at half-maxima, obtained by Gaussian fits) approaching to that of ZPL. This confirms that the PSB really monitors the exciton population as well as its spatial extension.

As discussed before, the HL peak monitors the individual coherence of the excitons. Thus the spatial profile of HL peak reflects the coherent propagation of excitons in space. We note that HWHM of the HL peak is related, but not equal, to the coherence length of the excitons, since both the excitation spot and the detection spot in our measurement are not given by delta functions in space. Using Monte Carlo simulations for deconvolution, we deduce that in our experimental setup the measured HWHM of the HL peak profile is actually 1.35 times the coherence length.

Figure 4 shows the coherence lengths measured in this way for several exciton kinetic energies by tuning the photon energy of the excitation laser. Increasing the exciton kinetic energy we find a slow drop of the coherence length. The decrease is less than 20 % as the kinetic energy is increased from 1.6 to 20.7 meV. We also show in the same figure (dots) the coherence length calculated by only considering the acoustic phonon scattering. For this estimation, the influence of static disorder is not considered, thus the exciton is assumed to propagate ballistically before the first acoustic phonon scattering event. The coherence length is thus calculated by simply multiplying the group velocity obtained from a parabolic dispersion and the acoustic phonon scattering time[31]. The discrepancy observed in Fig. 4 suggests that the excitonic propagation is limited by not only the acoustic phonon scattering but also other mechanisms like static disorder. The importance of the disorder on excitonic properties of semiconductor quantum wells at low temperature has

been proven (see, e.g., Ref. [32]). Recently, theoretical investigation[33] suggested a strong influence of disorder on the spatiotemporal dynamics of excitons in quantum wells under near-field pulsed excitation. Strong disorder can eventually results in exciton localization. Here, we are dealing with excitons with rather high kinetic energy above the effective mobility edge. A detailed theoretical study on the influence of static disorder on the coherence length of excitons is beyond the scope of the present investigation. However, Fig. 4 provides an important input for this kind of studies. We also note that the coherence length determined from the present investigation ($300 \sim 400$ nm) is about $25 \sim 30$ times the de Broglie wavelength of the exciton in ZnSe quantum wells.

In summary, we show that the combination of a highly efficient, sub- μm spatially resolved photoluminescence system with phonon sideband spectroscopy enables one to investigate coherence transport process in semiconductors. By monitoring the spatial evolution of the exciton coherence, we directly determine the exciton coherence length of $300 \sim 400$ nm, which decreases slowly when increasing the exciton kinetic energy.

We gratefully acknowledge the growth of excellent samples by the group of M. Heuken (RWTH Aachen) and useful discussion with H. Giessen (Universität Bonn) and R. von Baltz (Universität Karlsruhe). This work was supported by the Deutsche Forschungsgemeinschaft.

- [1] A. P. Heberle, J. J. Baumberg, and K. Köhler, *Phys. Rev. Lett.* **75**, 2598 (1995).
- [2] N. H. Bonadeo, J. Erland, D. Gammon, D. Park, D. S. Katzer, and D. G. Steel, *Science* **282**, 1473 (1998).
- [3] G. Chen, N. H. Bonadeo, D. G. Steel, D. Gammon, D. S. Katzer, D. Park, and L. J. Sham, *Science* **289**, 1906 (2000).
- [4] D. D. Awschalom and J. M. Kikkawa, *Phys. Today* **52**(6), 33 (1999).
- [5] V. V. Mitin, V. A. Kochelap, and M. A. Stroscio, *Quantum heterostructures* (Cambridge University Press, UK, 1999), p. 18.
- [6] P. A. Lee and T. V. Ramakrishnan, *Rev. Mod. Phys.* **57**, 287 (1985).
- [7] J. Shah, *Ultrafast spectroscopy of semiconductors and semiconductor nanostructures* (Springer, Germany, 1996), chap. 2.
- [8] D. Gammon, E. S. Snow, B. V. Shanabrook, D. S. Katzer, and D. Park, *Science* **273**, 87 (1996).
- [9] J. R. Guest, T. H. Stievater, G. Chen, E. A. Tabak, B. G. Orr, D. G. Steel, D. Gammon, and D. S. Katzer, *Science* **293**, 2224 (2001).
- [10] D. Sanvitto, F. Pulizzi, A. J. Shields, P. C. M. Christianen, S. N. Holmes, M. Y. Simmons, D. A. Ritchie, J. C. Maan, and M. Pepperd, *Science* **294**, 837 (2001).
- [11] M. Vollmer, H. Giessen, W. Stolz, W. W. Rühle, L. Ghislain, and V. Elings, *Appl. Phys. Lett.* **74**, 1791 (1999).
- [12] J. Hetzler, A. Brunner, M. Wegener, S. Leu, S. Nau, and W. Stolz, *Phys. Stat. Sol. B* **221**, 425 (2000).

- [13] M. Umlauff, J. Hoffmann, H. Kalt, W. Langbein, J. M. Hvam, M. Scholl, J. Söllner, M. Heuken, B. Jobst, and D. Hommel, Phys. Rev. B **57**, 1390 (1998).
- [14] K. Siantidis, V. M. Axt, and T. Kuhn, Phys. Rev. B **65**, 035303 (2002).
- [15] P. W. M. Blom, P. J. van Hall, C. Smit, J. P. Cuypers, and J. H. Wolter, Phys. Rev. Lett. **71**, 3878 (1993).
- [16] S. Permogorov, in *Excitons*, edited by E. I. Rashba and M. D. Sturge (North-Holland, Netherlands, 1982), chap. 5.
- [17] S. Permogorov, Phys. Stat. Sol. B **68**, 9 (1975).
- [18] Y. R. Shen, Phys. Rev. B **9**, 622 (1974).
- [19] J. R. Solin and H. Merkelo, Phys. Rev. B **12**, 624 (1975).
- [20] Y. R. Shen, Phys. Rev. B **14**, 1772 (1976).
- [21] J. R. Solin and H. Merkelo, Phys. Rev. B **14**, 1775 (1976).
- [22] R. P. Stanley, J. Hegarty, R. Fischer, J. Feldmann, E. O. Göbel, R. D. Feldman, and R. F. Austin, Phys. Rev. Lett. **67**, 128 (1991).
- [23] N. Pelekanos, J. Ding, Q. Fu, A. V. Nurmikko, S. M. Durbin, M. Kobayashi, and R. L. Gunshor, Phys. Rev. B **43**, 9354 (1991).
- [24] D. Some and A. V. Nurmikko, Phys. Rev. B **48**, 4418 (1993).
- [25] S. S. Prabhu, A. S. Vengurlekar, and J. Shah, Phys. Rev. B **53**, 10465 (1996).
- [26] R. Nötzel, L. Däweritz, N. N. Ledentsov, and K. Ploog, Appl. Phys. Lett. **60**, 1615 (1992).
- [27] I. G. Ivanov, T. Egilsson, Å. Henry, B. Monemar, and E. Janzén, Phys. Rev. B **64**, 085203 (2001).
- [28] H. Zhao, S. Moehl, S. Wachter, and H. Kalt, Appl. Phys. Lett. **80**, 1391 (2002).
- [29] M. Vollmer, H. Giessen, W. Stolz, W. W. Rühle, A. Knorr, S. W. Koch, L. Ghislain, and V. Elings, J. Microscopy **194**, 523 (1999).
- [30] G. von Freymann, D. Lüerßen, C. Rabenstein, M. Mikolajczyk, H. Richter, H. Kalt, T. Schimmel, M. Wegener, K. Okhawa, and D. Hommel, Appl. Phys. Lett. **76**, 203 (2000).
- [31] T. Takagahara, Phys. Rev. B **31**, 6552 (1985).
- [32] S. D. Baranovskii, U. Doerr, P. Thomas, A. Naumov, and W. Gebhardt, Phys. Rev. B **48**, 17149 (1993).
- [33] B. Hanewinkel, A. Knorr, P. Thomas, and S. W. Koch, Phys. Rev. B **60**, 8975 (1999).